


To Pay or Not to Pay Attention: Classifying and Interpreting Visual Selective Attention Frequency Features

Lora Fanda ¹[0000-0003-3432-3353], Yashin Dicente Cid²[0000-0001-7742-5363]
, Pawel J. Matusz^{1,*}[0000-0003-1721-4868], and
Davide Calvaresi^{1,*}[0000-0001-9816-7439]

¹ University of Applied Sciences Western Switzerland (HES-SO), Sierre, Switzerland
{lora.fanda,pawel.matusz,davide.calvaresi}@hevs.ch

² University of Warwick, Coventry, United Kingdom
yashin.dicente@warwick.ac.uk

*the authors share an equal contribution

Abstract. Selective attention is the ability to promote the processing of objects important for the accomplishment of our behavioral goals (target objects) over the objects not important to those goals (distractor objects). Previous investigations have shown that the mechanisms of selective attention contribute to enhancing perception in both simple daily tasks and more complex activities requiring learning new information. Recently, it has been verified that selective attention to target objects and distractor objects is separable in the frequency domain, using Logistic Regression (LR) and Support Vector Machines (SVMs) classification. However, discerning dynamics of target and distractor objects in the context of selective attention has not been accomplished yet.

This paper extends the investigations on the possible classification and interpretation of distraction and intention solely relying on neural activity (frequency features). In particular, this paper (*i*) classifies *distractor objects* vs. *target object* replicating the LR classification of prior studies, extending the analysis by (*ii*) interpreting the coefficient weights relating to all features with a focus on N2PC features, and (*iii*) retrains an LR classifier with the features deemed important by the interpretation analysis.

As a result of the interpretation methods, we have successfully decreased the feature size to 7.3 % of total features –i.e., from 19,072 to 1,386 features – while recording only a 0.04 loss in performance accuracy score – i.e., from 0.65 to 0.61. Additionally, the interpretation of the classifiers’ coefficient weights unveiled new evidence regarding frequency which has been discussed along with the paper.

Keywords: EEG, selective attention, machine learning.

1 Introduction

The comprehension of spatiotemporal brain dynamics can help identify selective attention in both healthy and attention-impaired individuals.

Humans' mental capacity to attend to and process in-depth the incoming information is limited [1]. According to Posner and Peterson [2], attention comprises three subsystems: (i) alerting, (ii) orienting, and (iii) selective attention. The latter is a naturally multisensory set of processes that flexibly engage the limited computational resources according to the task demands. Processing resources are scarce, and the stimuli received by the senses compete for them. Some theories (i.e., *biased-competition* [3]) detailed how the competition for resources is resolved and integrated across different brain processing stages, producing a coherent behavior.

Understanding such concepts requires both Neuroscience and Artificial Intelligence (AI) domain knowledge, with particular emphasis on Machine Learning (ML). The cognitive orchestration of selective attention, its role in enhancing perception & learning skills, and neurocognitive processes engaged by distractor *or* target objects have been widely investigated [4–6]. However, brain mechanisms and classification methods to distinguish selective attention to *target* vs. *distractor* objects have not been understood yet.

Achieving such an understanding can provide essential insights into functional differences in cortical cognitive mechanisms governing attention to object task-relevant and task-irrelevant. Therefore, understanding when and how well individuals pay attention to objects and events can lead to practical tools to better measure attention in the classroom or the workplace (if the ethical issues related to performance tracking vs. privacy are sufficiently addressed).

Current approaches adopt a cortical correlate of the attentional selection, known as the N2PC, of both targets and distractors possessing target features. N2PC is defined as a negative polarity at 200ms latency appearing over posterior electrodes contralateral to the direction of attention. In other words, the N2PC is reflected by enhanced negativity emerging approximately (200ms) after stimulus onset over posterior electrodes contralateral to the stimulus location. This measure uses neural signals derived from the acquired electroencephalogram (EEG) to identify selective attention to visual objects. The N2PC is obtained from EEG data via the event-related potential (ERP) technique involving averaging brain responses elicited by one type of stimulus over multiple repetitions of it over time. The averaging amplifies the faint neural signal reflecting neurocognitive processing of that stimulus. The N2PC is known to be particularly modulated by goal-based (“top-down”) and visual selective attention processes. Therefore, selective attention is measured in the window between approximately 150ms and 300ms after stimulus onset and lasts until the difference between the negative potential between hemispheres is no longer measured.

As of today, the analysis of selective attention via the traditional N2PC analytical approach is a human-intensive task, and as such, it is time-consuming, requires in-depth experience, and is currently not semi-automated [7]. Moreover, due to the high temporal resolution of the EEG signal, human-related errors (i.e., variability in the identification of the start and end of the N2PC time window) can jeopardize the results' precision and accuracy. Prior work has shown that attention to targets and distractors *is* separable in EEG via a classification

methodology using linear and non-linear classifiers [8]. However, the classification mentioned above has not been interpreted, leaving incomprehensible *which EEG frequency features* provide the most separable information.

This paper analyzes and interprets the frequency features using the same dataset employed in [8]. In particular, the classifiers' coefficient weights are interpreted to understand which features convey the most relevant information for classification. Finally, we discuss the relevance of our findings within the Neuroscience domain.

The rest of the paper is organized as follows. Section 2 presents the current state of the art about the many mechanisms and abstractions supporting our notion of attention, which is then introduced, defined, and discussed in section Section 3. Section 4 elicits the opportunities and presents the challenges related to our definition of attention. Finally, Section 5 concludes the paper.

2 State of the Art

The contribution of this paper relies on concepts intersecting neuroscience and machine learning. Therefore, this section provides the necessary background concepts and the related state of the art to facilitate the reader's comprehension of the topic.

EEG: Selective attention has been studied using various modes of data collection, ranging from invasive techniques like electrocorticography (ECoG) [9], to noninvasive techniques like EEG [10, 1]. Processes related to attention have distinct markers in the frequency domain [11, 12]. Therefore, EEG and ECoG are the preferred data acquisition techniques due to their high temporal resolutions and ability to detect these forms of attention-relevant oscillatory activity. Overall, EEG is preferred to ECoG as it is noninvasive and more convenient for collecting large amounts of electrophysiological data. Thus, EEG neural recordings can be used to classify selective attention to distractor objects, target objects, or non-object stimuli.

N2PC: In traditional methods, selective attention to potentially task-relevant objects is measured through N2PC. N2PC, an event-related potential (ERP) correlate, is a cortical measure of attention to candidate target objects in selective attention task contexts. On the one hand, for target objects, Nobre et al. [13] confirm the presence of changes in the ERP strength over the N2PC period triggered by visual target objects where attention has been captured by visual targets. On the other hand, the target object's properties can be the driving force that determines selective attention to *distractors*. This has been initially shown in behavioral responses in a study by Folk et al. and then confirmed in an EEG study by Eimer et al. [14] and further supported by multiple studies since since [15, 14]. Therefore, like for the target objects, N2PC is a well-used measure of selective attention for distractor objects. Hence, the N2PC is well suited as a marker of attending towards visual stimuli of distracting and task-relevant (target) type.

Frequency Components of Attention: Attention has a distinct imprint in the frequency domain. Thus, each frequency domain is associated with a class of attentional processing. Changes in the δ band power, $0.5 - 4 Hz$, allow for separation of low and high cognitive load while the θ band power reflects the encoding of new information. The α band power, $8 - 12 Hz$, is higher for target object perception during the attention task. The β band power, $13 - 30 Hz$, increases preceding the correct response. The γ band power, $30 - 70 Hz$, increases by a visual search task when the subject attends to a stimulus [16, 17]. Labeling each frequency band with one functionality can be misleading. Thus the range of these frequency bands will be considered as attention-relevant frequency bands.

Discrete Cosine Transform (DCT): A method for frequency feature extraction is the Discrete Cosine Transform (DCT). DCT extraction has previously been used for EEG and MEG datasets [18, 19] to extract frequency components of a signal to use in classification. Table 1 summarized ranges of EEG frequency bands and related DCT ranges for convenience.

Frequency Bands						
	δ	θ	α	β	γ	high γ
Frequency Range (Hz)	(0.5-4)	(4-8)	(8-13)	(13-30)	(30-50)	(50-80)
DCT Range	[1:2]	[2:3]	[3:5]	[5:10]	[10:17]	[15:25]

Table 1. Table of Frequency bands in EEG datasets and their translation to DCT for our EEG dataset.

Classifying Neural Data: In the fields of Brain-Computer Interfaces (BCIs) and Epileptic seizure detection, the interest in the classification of neural data is growing. The most common features used in the classification of BCI and Epilepsy data are raw EEG, frequency component extraction, and AutoRegressive features [20, 21]. In comparison, the most common features to classify selective attention are raw EEG, frequency component, and N2PC electrode features [22].

Logistic regression (LR) recorded promising performance accuracy for classification of biological brain signals [8, 20, 23-25]. LR is generally used as a categorical problem-solving method, thus can be applied to multivariate classification [26]. It is deemed a simpler classification technique but can provide unique results if feature vectors are adequately selected and if the data is linearly separable. It is important to note that, unlike BCI/Epilepsy classification applications, selective attention classification had only recently been applied, and it is a steadily growing field.

Classification of Attention Data: Fanda verified that selective attention is separable in the frequency domain using LR and SVM classification and, from manual feature selection, showed that N2PC region electrodes hold the most discriminative information compared to non-N2PC regions [8]. However, in such a study, comparisons across low to high-frequency features are lacking,

and the coefficient weights relating to the features have not been interpreted, thus undermining the understanding of the classifier decision-making.

Contribution: In light of the findings mentioned above and due to the lack of interpretability in DCT feature classification of selective attention data, this paper *(i)* replicates the LR classification performed in [8], *(ii)* interprets the coefficient weights relating to all features with a focus on N2PC features, and *(iii)* retrains an LR classifier with the features deemed important by the interpretation analysis.

3 Approach or Method

Overall, to interpret the selective attention frequency features, we will replicate the classification using LR, interpret the model’s weights, and retrain the classifier with sub-selected features as extracted from the interpretation data. To facilitate the reader’s comprehension, Figure 1 summarizes the overall pipeline spanning from the EEG data acquisition to the performance analysis. In particular, Figure 1 (a) explicates the step undertaken in prior work, such as EEG dataset and N2PC analysis division [15], and DCT feature extraction and initial LR classification parameters [8]. Figure 1 (b) organizes the tasks and results obtained in the specific phases (PHx) of this study, such as (PH1) replication of the initial LR classification, (PH2) interpretation of the features contributing the most information to the replicated LR classifiers’ coefficient weights for all features, (PH3) re-learning LR classification with sub-selected featured as extracted by R1, and (PH4) performance assessment and comparison of all LR classifiers.

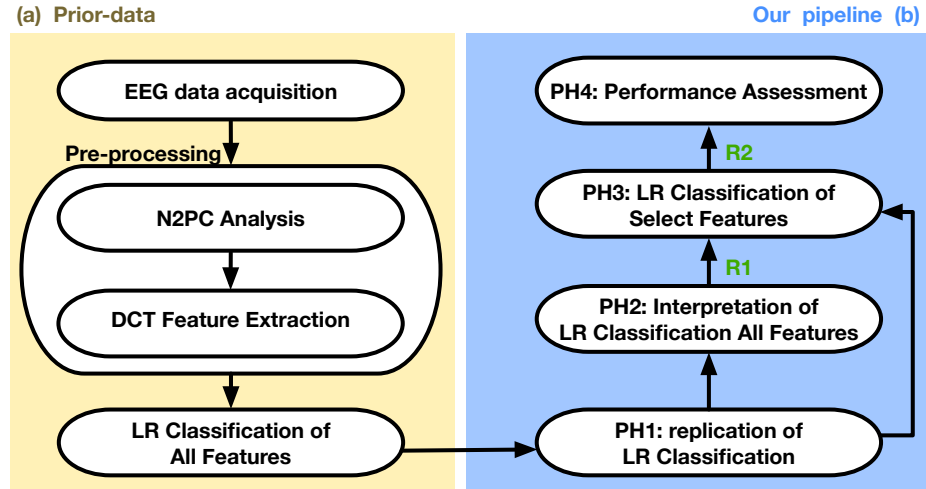


Fig. 1. Overall pipeline from data acquisition to performance analysis: (a) prior work’s tasks, (b) methodology pipeline of this contribution.

EEG Data Acquisition: The EEG dataset has been collected using a 129-channel HydroCel Geodesic Sensor Net connected to a NetStation amplifier (Net Amps 400; Electrical Geodesics Inc., Eugene, OR, USA) where 128 electrodes have been used at a 1 kHz sampling rate. During data acquisition, electrode impedances have been kept below $50k\Omega$, and electrodes have been referenced online to Cz, a common reference for EEG cap data collection. Participants have been recorded for three hours in a task described in Turoman et al. [15]. This dataset has been collected by Dr. Turoman during her Ph.D. work [27]. To complete the task, the participants have been instructed to search for a predefined color target (target object) in a search array and report the target’s orientation (i.e., if the target is horizontal, press right, otherwise, press left). The participants have been instructed about other objects that could appear (distractor objects) and focus solely on reporting the target’s orientation. Figure 2 shows examples of the task.

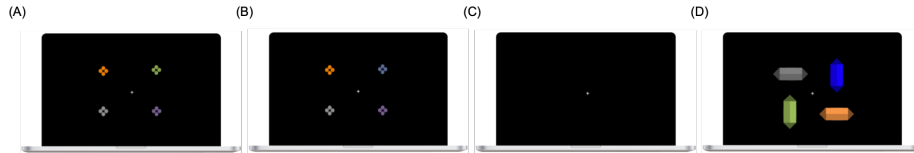


Fig. 2. This figure shows all four stimuli of the paradigm (A - D) and the time importance of the three interested time-ranges. (A) is “Baseline” Class 0, (B) is “Cue” Class 1, and (D) is “Target” Class 2 stimuli. The cross (C) is not used in this study. Reproduced from Fanda [8].

Preprocessing: This paper extends the work done in [27]. Therefore, it is worth recalling that data have been band-pass filtered between $0.1 Hz$ and $40 Hz$, notch filtered at $50 Hz$, and Butter-Worth filtered of phase shift elimination at $-12 dB/octave$ roll-off. Automatic artifact rejection of ± 100 micro-Volts has been used to increase the signal-to-noise ratio. Next, trials have been segmented to separate base, distractor, and target array neural responses for feature extraction.

N2PC Analysis: In [15], the authors have applied N2PC to the dataset in analysis and successfully computed selective attention activity to distractors. Figure 3 (A) shows N2PC activity from 180 to 300 ms time range for a visual (TCCV) and audiovisual (TCCAV) property of the stimuli. Figure 3 (B) shows the region of N2PC electrode coverage (in red), which is a collection of 14 electrodes around the two main N2PC electrodes (e65 and e90). In this paper, N2PC electrodes refer to the 14 electrodes in the N2PC region from the TCCV condition only, as shown in Figure 3 (B).

DCT of N2PC Time-Frame: DCT decomposes and compresses a signal to ($signal-length - 1$) frequency bins. The benefit of using DCT features relies on

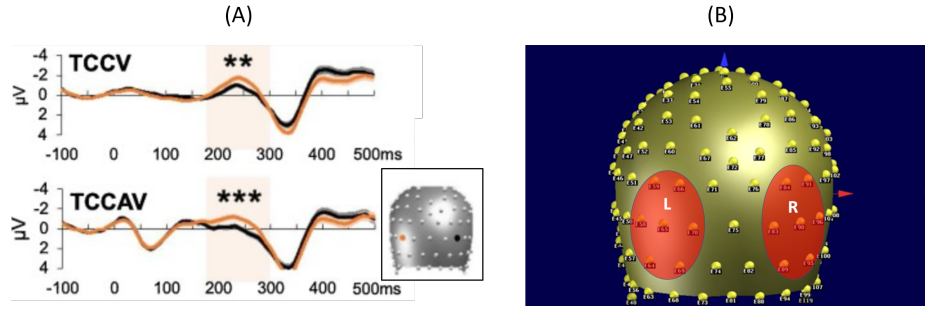


Fig. 3. N2PC analysis: (A) N2PC analysis, indicating presence of N2PC from ~ 200 to ~ 300 ms (taken from Turoman et al. [15]). (B) EEG Cap images referencing N2PC region electrodes, taken from Fanda [8].

containing the full frequency identity of the signal while removing biases that can come from time-series and amplitude measures. Equation 1 is one-dimensional DCT, and it is used for feature extraction.

$$y_k = 2 \sum_{n=0}^{N-1} x_n \cos\left(\frac{\pi k(2n+1)}{2N}\right) \quad (1)$$

For example, if a signal x_n is sampled at 1024 Hz for a length of $N = 150$, the frequency components extend up to 512 Hz . When applying DCT, the 512 Hz frequency components of the signal are cosine-transformed into $(N-1) = 149$ frequency bins, keeping only the real values of the signal. This results in the y_k vector where the first value $k = 0$ contains prevalence via summation of frequencies ranging from 0 to 3.33 Hz , the second bin from 3.34 to 6.66 Hz , and so on.

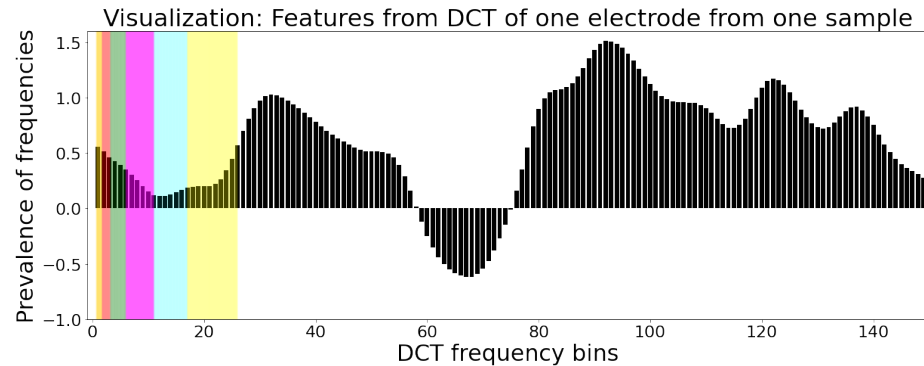


Fig. 4. DCT features visualized for one electrode of one training sample. The shaded regions correspond to frequencies, as translated from Table 1.

Prior knowledge of attentional frequency oscillation dictates that selective attention primarily ranges from 8 Hz to 30 Hz (attention relevant frequency band) [10]. For the DCT extraction of the dataset, this range is contained in DCT bins one to 27 (see Figure 4). Thus, the lower DCT bins likely contain more relevant information to selective attention than the higher bins. Such a hypothesis is tested by looking at the coefficients of the features in our learned classifier’s decision function.

Classification: In this paper, we aim to classify and interpret selective attention EEG data. Specifically, we used LR to classify *distractor objects* vs. *target object*, and interpret the classifier feature coefficient weights. With LR, we used a one-vs-all multi-class structure. The features used for the LR classifier are normalized DCT features, split by participant into train, validation, and test sets. To evaluate the model, performance accuracy scores have been used as a performance evaluation technique.

Interpretability of LR: In this contribution, interpretability approaches are applied to classifiers to examine the contribution of individual predictors. One method consists of the examination of the regression coefficients of each of the three LR classifiers resulting from our multi-class problem using a one-vs-all setup. LR coefficients are slightly more difficult to interpret as the line of best fit is a **logit** function, the inverse of the sigmoid curve. Thus, the resulting coefficients of LR are *odds ratios* and require exponentiation to convert to regular odds. The odds ratio then corresponds to the β_k coefficients where $k \in [1, n]$ with $n = \text{total predictors}$ in the LR odds equation 2, where x ’s are values of predictors.

$$\frac{\text{odds}(x_1 + 1)}{\text{odds}(x_1)} = \frac{e^{\beta_0 + \beta_1(x_1+1) + \beta_2x_2 + \dots + \beta_nx_n}}{e^{\beta_0 + \beta_1x_1 + \beta_2x_2 + \dots + \beta_nx_n}} = \frac{e^{\beta_1(x_1+1)}}{e^{\beta_1x_1}} = e^{\beta_1} \quad (2)$$

Post conversion, the values of the coefficients are positive, and they are interpreted following the rule below:

$$\text{Odds} = \begin{cases} e^{\beta_k} \times \text{as likely,} & \text{if } e^{\beta_k} \geq 1 \\ \frac{1}{e^{\beta_k}} \times \text{as unlikely,} & \text{if } e^{\beta_k} < 1 \end{cases} \quad (3)$$

As an example, taking $k=1$ coefficient β_1 from class A , this rule roughly translates to:

- for $e^{\beta_1} \geq 1$: “Each unit increase in x_1 , the odds that the observation is in class A are e^{β_1} times as likely as the odds that the observation is not in A .”
- for $e^{\beta_1} < 1$: “Each unit increase in x_1 , the odds that the observation is NOT in class A are $\frac{1}{e^{\beta_1}}$ times as *unlikely* as the odds that the observation is in A .”

4 Results & Discussions

This section describes the two main results: (R1) the interpreted LR classifiers’ coefficient weights as odds ratios for *all* features and N2PC features and (R2) the

LR classification accuracy score comparison, using all, N2PC only, and N2PC & selected DCT features. Additionally, the discussions are included in the end.

R1 - Coefficient Weights as Odds Ratios: All features and N2PC: It is worth recalling that due to the one vs. rest multi-class choice of LR classification, each class has a set of odds ratios extracted from the model’s coefficients weights. Thus, the analyses are shown for each classifier (Baseline, Distractor, or Target) individually. To inspect if N2PC electrodes have information *more* valuable than other electrodes to the decision function of the classifier, we have plotted in Figure 6 the odds ratios of classifiers for Baseline (brown), Distractor (blue), and Target (purple), where the N2PC region electrodes are plotted using a darker color for contrast.

From Figure 5, N2PC electrodes overall have higher odds ratios compared to other electrodes. To better see the pattern of the distinct shape of the N2PC electrodes, we stacked the coefficient weights vector with respect to DCT frequency bin features, resulting in a 128 by 149 coefficient matrix as plotted in Figure 6 for each classifier. In addition to identifying the distinct N2PC electrode patterns, we can understand in *which* DCT bins the odds ratios across the

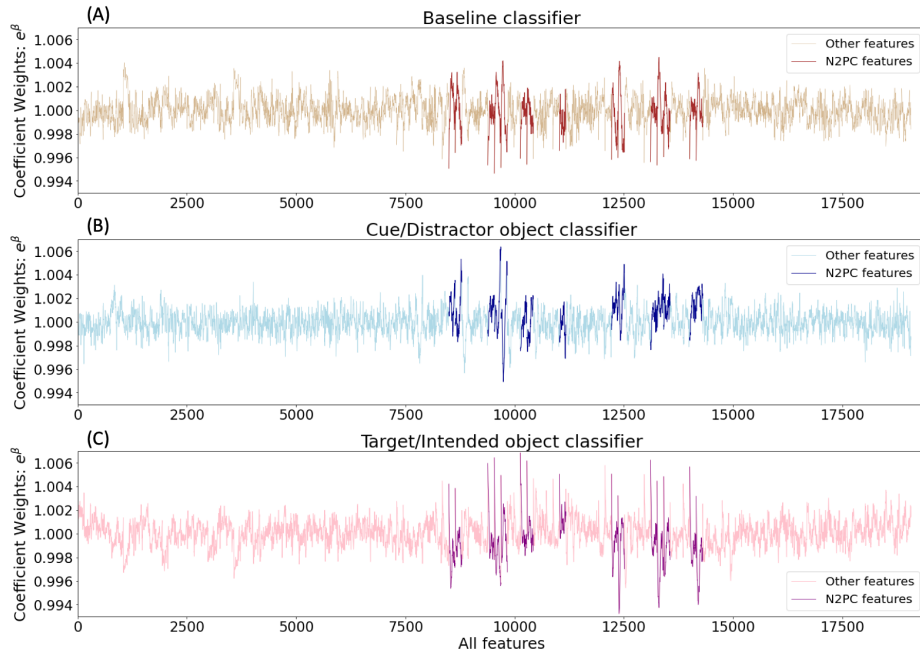


Fig. 5. Coefficients as odds ratios of the features in the decision function of LR classification. In all three classifiers above, for each class, the N2PC electrodes visibly have higher peaks. Figure 6 stacks the feature vector by electrode to better visualize the patterns with respect to DCT frequency bins.

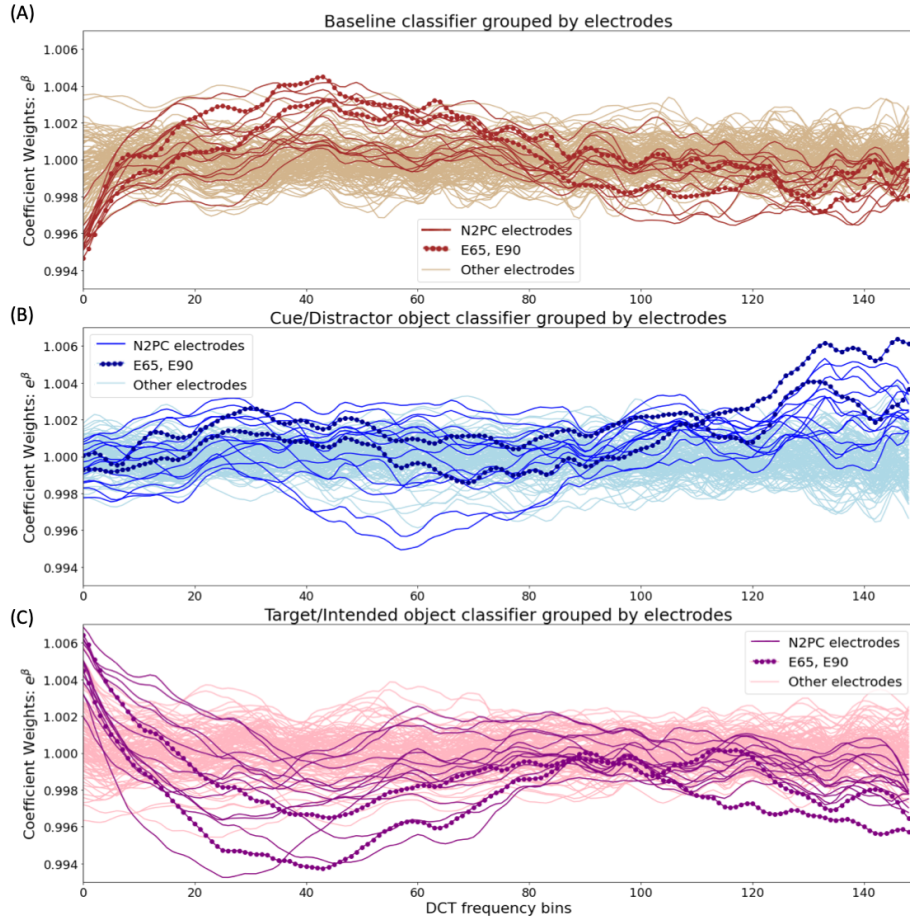


Fig. 6. Coefficients as odds ratios of the features in the decision function of LR, organized by electrode: This figure reorganizes the coefficient weights seen in figure 5 by stacking them electrodes (to highlight the patterns w.r.t. DCT frequency bins). The coefficient weights, as odds ratios, are plotted for (A) Baseline, (B) Cue, and (C) Target classifiers. The N2PC electrodes are highlighted in a darker color to show the difference in patterns over DCT frequency bins. E65 and E90 are further highlighted because they are the selective electrodes studied by Turoman et al. [15], from whom the dataset was taken.

three classifiers diverse/stay similar. Then, the odds ratios are analyzed using equation 2.

In particular, each unit increase in DCT 1 to 3, the odds that the observation is in-class Target is $\beta_{1-3} \in (\sim 1.004, \sim 1.006)$ times as likely as the odds that the observation is not in class Target. Conversely, each unit increase in DCT, the odds that the observation is *not* in class Target is $\frac{1}{\beta} = \frac{1}{0.995} = 1.005$ times as likely as the odds that the observation is in class Target. Following this rule,

we set a threshold of 1.000 ± 0.004 for selecting the DCT components for future analysis. A visualization of this threshold is seen in Figure 7. All DCT features with odds ratio values falling below 0.996 and above 1.004 have been selected for the next iteration of LR classification. This resulted in the selection of the following DCT regions:

Baseline: DCTs [49:71 and 125:149]
 Distractor: DCTs [0:5 and 32:51]
 Target: DCTs [0:72 and 140 - 149]

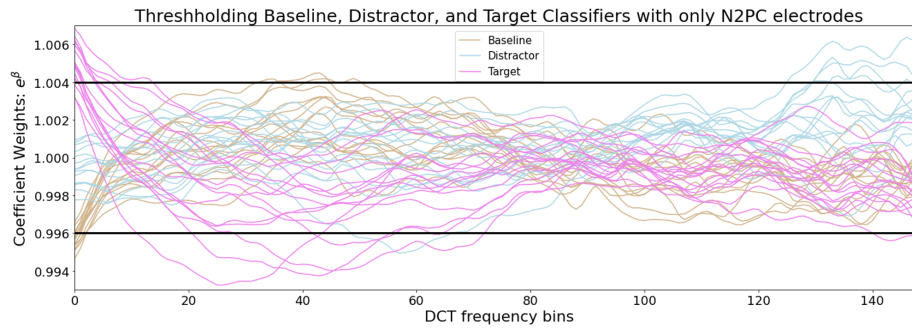


Fig. 7. DCT threshold visualization for DCT feature selection for interpreting which DCT features among N2PC region electrodes are more important. Here, the common denominator of DCT ranges across all three classifiers is DCT 0 to 73 and 124 to 149.

As a result, in the next iteration of LR classification, only the N2PC region features, and DCT features 0 to 73 and 124 to 149 will be used. The rest of the features will be discarded.

Coefficient Weight analysis for N2PC electrode features: To analyze the weight of the coefficients for N2PC electrode features, we used the conversion in Table 1. Frequency bands relating to selective attention activity will not be defined in purpose. Nevertheless, it is known that these frequency ranges' power can correlate with selective attention activity. As such, we expect the odds ratios to have a visibly higher or lower value than 1 for DCT frequency bins from 1 to 27. Taking threshold 1.004 and 0.996, we retrained the LR and compared the performance accuracy scores between all features, only N2PC but all DCTs, and only N2PC and selected DCT.

Confusion Matrices: To compare the performance of the three iterations of learning an LR classifier, accuracy scores and confusion matrices are reported in Figure 8. Confusion matrices have been calculated to understand better the intra-class classification accuracy and errors for (A) All features, (B) N2PC region features with all DCT components, and (C) N2PC region features with selected DCT components.

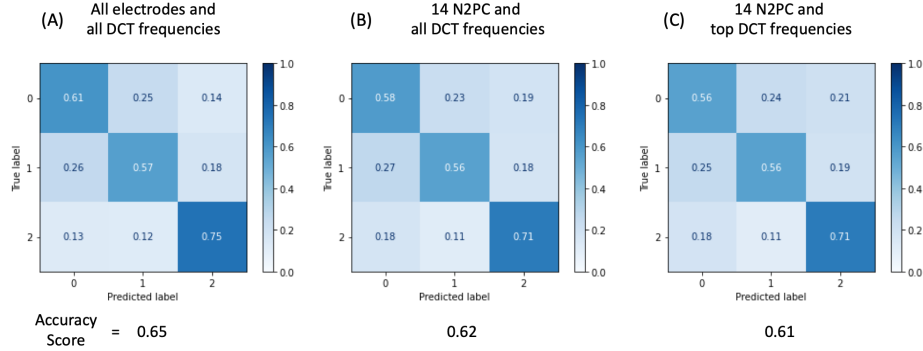


Fig. 8. Confusion Matrices of LR classification accuracy scores using (A) all features, (B) N2PC region features, and (C) N2PC region and select DCT features. The accuracy scores are shown for each class true labels (y axis) and predicted labels (x axis), for Baseline (Class 0), Cue (Class 1), and Target (Class 2). The overall classifier accuracy is written in the bottom.

Discussions: In this work, we have analyzed the most valuable features of the LR classifier’s decision function. In line with what identified in [8], from manual feature selection, N2PC region electrodes hold the most discriminative information compared to non-N2PC regions. Lead by the lack of interpretability in DCT feature classification in EEG datasets, this paper (i) replicates the LR classification performed in [8], (ii) interprets the coefficient weights relating to all features with a focus on N2PC features, and (iii) retrains an LR classifier with the features deemed discriminant by the interpretation analysis.

We verified that N2PC region electrode features hold more discriminative information than non-N2PC region electrodes, as seen by Figure 6. Additionally, we have identified that DCT frequencies of zero to 73 and 123 to 149 held the most discriminative information than other DCT frequency bins, as seen by Figure 7. We retrained an LR classifier using only the sub-selection of features (i.e., $\frac{14 \cdot 99}{19072} = \frac{1386}{19072} = 7.3\%$ of the original features vector size), with only a 0.04 loss in performance accuracy score. Some of the expected outcomes from the interpretations are:

- E1.** N2PC region electrodes overall have higher odds ratios compared to other electrodes (Figure 5 (A-C)). This verifies that N2PC region electrodes have higher activity associated with selective attention.
- E2.** In the Baseline classifier, each unit increase in the DCT frequency bins 0 to 7 suggested that the odds that the features are **not** in the Baseline class are larger than the odds that the feature **is** in the Baseline Class (Figure 5 (A)). As DCT frequency bins zero to 7 correspond to selective attention frequencies, this confirms previous work. In other words, given values of < 1 in these regions, the odds ratio suggests that these selective attention

frequency values are discriminating that they do not belong in the Baseline classifier.

- E3.** In the Target classifier, each unit increase in the DCT frequency bins 0 to 7 suggested that the odds that the features are NOT in the Target class are larger than the odds that the feature *is* in the Target Class (Figure 5 (A)). As DCT frequency bins zero to 7 correspond to selective attention frequencies, this confirms previous work.

Additionally, some novel evidence can be extracted from the interpretation of the odds ratios in PH1 and PH2 (see Figure 1):

- E4.** The Distractor classifier odds ratios suggest that DCT features from 120 to 149 have high discriminability information. However, such high DCT frequency bins correspond to frequencies of 500 Hz. Thus, this requires more investigation as they could be related to artifacts (Figure 5 (B)).
- E5.** DCT frequency bins 20 to 80 have unexpectedly high odds ratios, which correspond to frequencies of 60 to 360 Hz. To the best of our knowledge, it suggests the presence of discriminating information in those frequency bands that have not been explained yet.

5 Conclusions

Prior work in classifying selective attention identifies the relevance on N2PC electrodes. However, they neglect feature interpretation. This study tackled the interpretation of LR classifiers to better discern the dynamics of target and distractor objects in the context of selective attention.

In particular, this paper has *(i)* classified *distractor objects* vs. *target object* replicating the LR classification of prior studies, *(ii)* interpreted the coefficient weights relating to all features with focus on N2PC features, and *(iii)* retrained an LR classifier with the features deemed important by the interpretation analysis.

The two main results of the interpretation methods are *(i)* successful feature size reduction (decreasing feature size to 7.3 % of total features –i.e., from 19072 to 1,386 features – while recording only a 0.04 loss in performance accuracy score), *(ii)* the interpretation of the classifiers’ coefficient weights unveiled new evidence.

In particular, such evidence are [E1.] N2PC region electrodes overall have higher odds ratios compared to non-N2PC electrodes; [E2.] In the Baseline classifier, each unit increase in the DCT frequency bins 0 to 7 suggested that the odds that the features are **not** in the Baseline class are larger than the odds that the feature **is** odds ratios of the Baseline classifier suggests that DCTs relating to Selective Attention frequency ranges are more *unlikely* to belong to Baseline class; [E3.] each unit increase in the DCT frequency bins 0 to 7 suggested that the odds that the features are the Target class are larger than the odds that they are not in the Target class.

Future works include the investigation of [E4] high DCT frequency bins having the most discriminant information for Distractor classifiers and [E5] DCT bins from 20 to 80 (approximately 60 - 360 Hz) having high odds ratios for all classifiers. It is important to understand the nature of the DCT components in relation to selective attention frequencies.

References

1. Marisa Carrasco. Visual attention: The past 25 years. *Vision research*, 51(13):1484–1525, 2011.
2. Michael I Posner and Steven E Petersen. The attention system of the human brain. *Annual review of neuroscience*, 13(1):25–42, 1990.
3. Robert Desimone and John Duncan. Neural mechanisms of selective visual attention. *Annual review of neuroscience*, 18(1):193–222, 1995.
4. Monika Kiss, José Van Velzen, and Martin Eimer. The n2pc component and its links to attention shifts and spatially selective visual processing. *Psychophysiology*, 45(2):240–249, 2008.
5. Micah M Murray, Antonia Thelen, Gregor Thut, Vincenzo Romei, Roberto Martuzzi, and Pawel J Matusz. The multisensory function of the human primary visual cortex. *Neuropsychologia*, 83:161–169, 2016.
6. Pawel J Matusz, Suzanne Dikker, Alexander G Huth, and Catherine Perrodin. Are we ready for real-world neuroscience?, 2019.
7. Ruxandra I Tivadar and Micah M Murray. A primer on electroencephalography and event-related potentials for organizational neuroscience. *Organizational Research Methods*, 22(1):69–94, 2019.
8. Lora Fanda. Classifying attentional dynamics from eeg signals: Feature based perceptual attentional control, February 2021.
9. Jennifer Shum, Lora Fanda, Patricia Dugan, Werner K. Doyle, Orrin Devinsky, and Adeen Flinker. Neural correlates of sign language production revealed by electrocorticography. *Neurology*, 95(21):e2880–e2889, 2020.
10. Monika Kiss, Anna Grubert, Anders Petersen, and Martin Eimer. Attentional capture by salient distractors during visual search is determined by temporal task demands. *Journal of cognitive neuroscience*, 24(3):749–759, 2012.
11. Wolfgang Klimesch. Alpha-band oscillations, attention, and controlled access to stored information. *Trends in cognitive sciences*, 16(12):606–617, 2012.
12. Francesca Marturano, Sabrina Brigadoi, Mattia Doro, Roberto Dell’Acqua, and Giovanni Sparacino. A time-frequency analysis for the online detection of the n2pc event-related potential (erp) component in individual eeg datasets. In *2020 42nd Annual International Conference of the IEEE Engineering in Medicine & Biology Society (EMBC)*, pages 1019–1022. IEEE, 2020.
13. Jennifer T Coull and Anna C Nobre. Where and when to pay attention: the neural systems for directing attention to spatial locations and to time intervals as revealed by both pet and fmri. *Journal of Neuroscience*, 18(18):7426–7435, 1998.
14. Charles L Folk, Roger W Remington, and James C Johnston. Involuntary covert orienting is contingent on attentional control settings. *Journal of Experimental Psychology: Human perception and performance*, 18(4):1030, 1992.
15. Nora Turoman, Ruxandra I Tivadar, Chrysa Retsa, Anne M Maillard, Gaia Scerif, and Pawel J Matusz. The development of attentional control mechanisms in multisensory environments. *Developmental cognitive neuroscience*, page 100930, 2021.

16. Francesca Marturano, Sabrina Brigadoi, Mattia Doro, Roberto Dell'Acqua, and Giovanni Sparacino. A time-frequency analysis for the online detection of the n2pc event-related potential (erp) component in individual eeg datasets. In *2020 42nd Annual International Conference of the IEEE Engineering in Medicine & Biology Society (EMBC)*, pages 1019–1022. IEEE, 2020.
17. Thomas Gruber, Matthias M Müller, Andreas Keil, and Thomas Elbert. Selective visual-spatial attention alters induced gamma band responses in the human eeg. *Clinical neurophysiology*, 110(12):2074–2085, 1999.
18. Seyed Mostafa Kia, Emanuele Olivetti, and Paolo Avesani. Discrete cosine transform for meg signal decoding. In *2013 International Workshop on Pattern Recognition in Neuroimaging*, pages 132–135. IEEE, 2013.
19. Mohammad Zavid Parvez and Manoranjan Paul. Features extraction and classification for ictal and interictal eeg signals using emd and dct. In *2012 15th International Conference on Computer and Information Technology (ICCIT)*, pages 132–137. IEEE, 2012.
20. Fabien Lotte, Marco Congedo, Anatole Lécuyer, Fabrice Lamarche, and Bruno Arnaldi. A review of classification algorithms for eeg-based brain–computer interfaces. *Journal of neural engineering*, 4(2):R1, 2007.
21. Md Khayrul Bashar, Faruque Reza, Zamzuri Idris, and Hiroaki Yoshida. Epileptic seizure classification from intracranial eeg signals: A comparative study eeg-based seizure classification. In *2016 IEEE EMBS Conference on Biomedical Engineering and Sciences (IECBES)*, pages 96–101. IEEE, 2016.
22. Johannes Jacobus Fahrenfort, Anna Grubert, Christian NL Olivers, and Martin Eimer. Multivariate eeg analyses support high-resolution tracking of feature-based attentional selection. *Scientific reports*, 7(1):1–15, 2017.
23. Fabien Lotte, Laurent Bougrain, Andrzej Cichocki, Maureen Clerc, Marco Congedo, Alain Rakotomamonjy, and Florian Yger. A review of classification algorithms for eeg-based brain–computer interfaces: a 10 year update. *Journal of neural engineering*, 15(3):031005, 2018.
24. Alois Schlögl, Felix Lee, Horst Bischof, and Gert Pfurtscheller. Characterization of four-class motor imagery eeg data for the bci-competition 2005. *Journal of neural engineering*, 2(4):L14, 2005.
25. Deon Garrett, David A Peterson, Charles W Anderson, and Michael H Thaut. Comparison of linear, nonlinear, and feature selection methods for eeg signal classification. *IEEE Transactions on neural systems and rehabilitation engineering*, 11(2):141–144, 2003.
26. Logistic regression: sklearn. https://scikit-learn.org/stable/modules/generated/sklearn.linear_model.LogisticRegression.html#sklearn.linear_model.LogisticRegression. Accessed: 2020-06-30.
27. Nora Turoman. *Early Multisensory Attention as a Foundation for Learning in Multicultural Switzerland*. PhD thesis, éditeur non identifié, 2020.